

The Effect of Thin Oxide Layers on Shallow Junction Formation

P.A. Stolk, J. Schmitz, F.N. Cubaynes, A.C.M.C. van Brandenburg, J.G.M. van Berkum,* and W.G. van der Wijgert*
Philips Research Laboratories, Eindhoven, The Netherlands

**CFT, Philips, Eindhoven, The Netherlands*

E-mail: stolk@natlab.research.philips.com

Abstract

This paper studies the influence of thin oxide screening layers on the formation of shallow junctions by low-energy B implantation and rapid thermal annealing. For screening oxides in the range from 0 to 10 nm, it is found that the trade-off between junction depth and sheet resistance (ρ_{sh}) is not affected as long as the implanted dose is adjusted to compensate for B trapping in the oxide. For a fixed implant dose and energy, however, minute variations in the oxide thickness have a large influence on ρ_{sh} , which limits the reproducibility of the junction formation process.

1. Introduction

The fabrication of PMOS transistors in advanced CMOS processes calls for ultrashallow p^+ junctions with increasingly low junction depth (X_J) while maintaining a low sheet resistance (ρ_{sh}). One route to achieving such shallow junctions lies in the use of B implantation at energies as low as 0.5-1 keV [1,2]. The electrical activation of these shallow implanted profiles is affected by the presence of thin oxide layers when the projected ion range R_p becomes of the order of the oxide thickness T_{ox} [3]. This is because a considerable portion of the

implanted B becomes trapped in the oxide. In CMOS processing, this situation occurs, for instance, during the implantation of source/drain extensions through the thin oxides remaining after poly-gate etching and reoxidation. In a recent paper [4], it has been shown that B trapping in the screening oxide is not necessarily detrimental, since the implanted oxides can serve as a diffusion source for junction formation.

In this paper, we study two aspects of B implantation in the presence of screening oxides. First, we systematically study the activation behavior of 1 keV B implants ($R_p \sim 5$ nm) for a range of oxide thicknesses ($T_{ox} \leq 10$ nm). In doing so, the full scope of junction formation strategies is covered, ranging from direct B implantation into Si ($R_p > T_{ox}$) to B out-diffusion from implanted oxides ($R_p < T_{ox}$). Second, we investigate how screening oxides affect the reproducibility of shallow junction formation by analyzing the impact of within-wafer T_{ox} variations on X_J and ρ_{sh} .

2. Experiment

Two types of screening oxides were grown on 6" Si wafers using dry oxidation in a horizontal tube furnace. The first set consisted of uniform oxide layers with thicknesses ranging from 0 (native oxide) to

10 nm. The second set consisted of non-uniform oxides, grown under perturbed gas flow conditions by leaving the furnace door open. This set enables an accurate analysis of the effect of small T_{ox} variations on junction formation. The wafers were implanted with 0.5 or 1 keV B to doses ranging from 3×10^{14} to $3 \times 10^{15}/\text{cm}^2$, and activated using rapid thermal annealing (RTA). Oxide thicknesses were measured using ellipsometry, while sheet resistances were obtained from four-point probe and Hall measurements. Secondary ion mass spectrometry (SIMS) was used to measure the B depth distribution $C_B(x)$ after diffusion, from which junction depths were derived using $C_B(X_J) = 10^{18}/\text{cm}^3$.

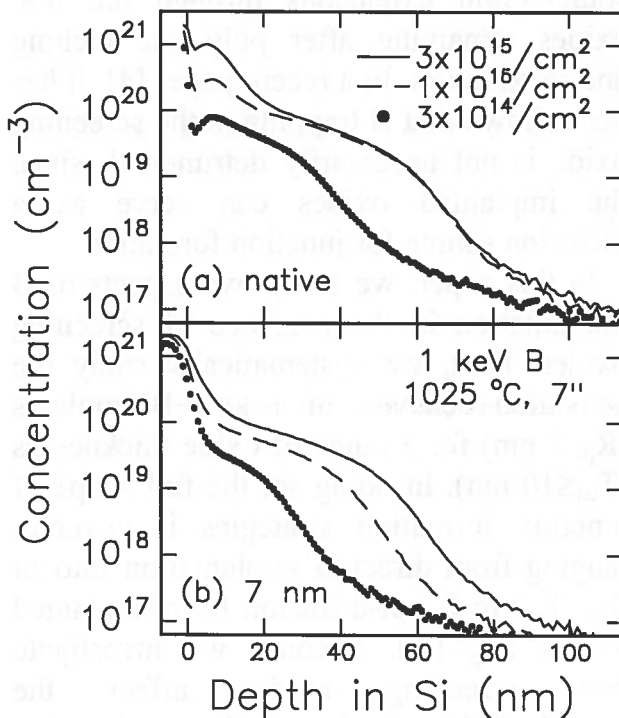


Figure 1. SIMS measurements of 1 keV B implants (various doses) annealed at 1025°C for 7 s in samples with (a) native and (b) 7-nm-thick screening oxides.

3. Results and discussion

Figure 1 shows the redistribution of a 1 keV B implant during annealing at 1025°C for 7 s in the presence of a native and a 7-

nm-thick screening oxide. For samples with a native oxide (Fig. 1a), increasing the implant dose from 3×10^{14} to $1 \times 10^{15}/\text{cm}^2$ leads to an increase in X_J as a result of concentration-enhanced diffusion. However, no further increase is seen upon raising the dose to $3 \times 10^{15}/\text{cm}^2$. This saturation arises from the clustering of the extra implanted B in the peak of the implanted profile (~ 5 nm deep), leading to the formation of immobile, inactive B agglomerates [1]. In the case of 7-nm-thick oxides (Fig. 1b), on the other hand, the peak portion of the 1 keV B implant is contained within the oxide layer (at $x < 0$ in Fig. 1). In this case, B out-diffusion from the oxide occurs. As a result, the B profile in the Si remains below the clustering level, and the incorporated B level and junction depth progressively increase with increasing dose.

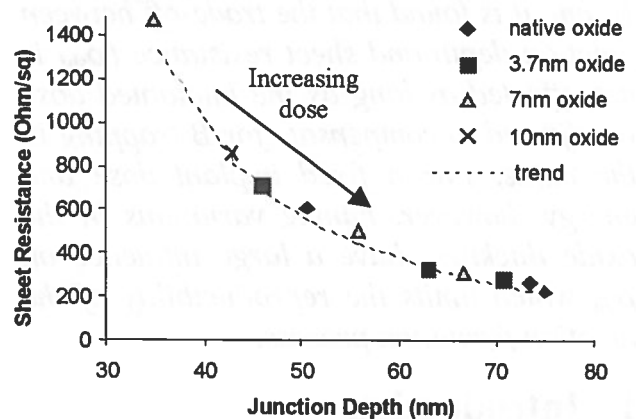


Figure 2. Sheet resistance vs. junction depth ($@C_B = 10^{18}/\text{cm}^3$) for 1 keV B implants annealed at 1025°C for 7 s. Data are shown for different screening oxides and implant doses.

Figure 1 demonstrates that, for a fixed implant dose, the trapping of implanted B in the screening oxide leads to a reduction in both the junction depth and the B level incorporated in the Si. Electrical measurements were performed to evaluate the trade-off between X_J and ρ_{sh} for various screening oxide thicknesses (Fig. 2). It is

clear that all samples follow the same trend of ρ_{sh} vs. X_J , independent of T_{ox} . This implies that reaching a certain target in X_J always yields the same ρ_{sh} , regardless of whether the shallow junctions are formed by direct implantation of B into Si, or by B in-diffusion from implanted oxides.

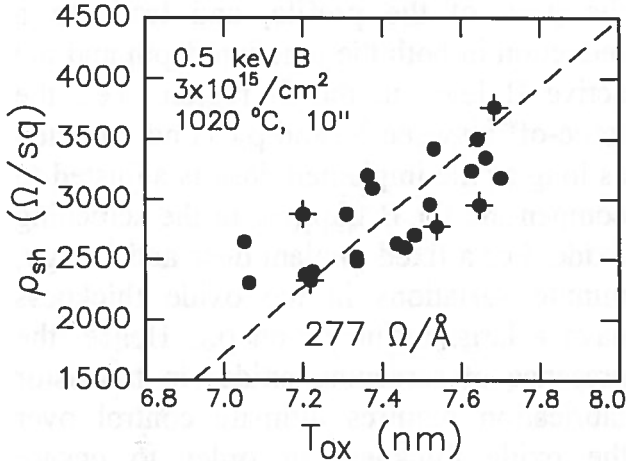


Figure 3. Correlation plots of ρ_{sh} vs. T_{ox} as obtained from wafer mapping of implanted and annealed wafers with non-uniform screening oxides. The points indicated by crosses were also analyzed by SIMS (Fig. 4).

While Fig. 2 indicates that screening oxides neither harm nor improve the shallow junction characteristics, the presence of thin oxide layers affect the reproducibility with which the junctions can be formed. In order to investigate this in detail, the dependence of ρ_{sh} on T_{ox} was accurately measured by means of wafer mapping. Figure 3 reveals a strong correlation between T_{ox} and ρ_{sh} (correlation coefficient $r=0.75$);¹ small variations in T_{ox} of <1 nm cause changes in ρ_{sh} of almost a factor of 2. In comparison, control measurements on samples with uniform oxides demonstrate that T_{ox} and ρ_{sh} are

¹ It was verified that the data scattering in the correlation plot of Fig. 3 is entirely caused by the inaccuracy of ellipsometry in determining the oxide thickness (standard deviation of 1.5 Å, as estimated from measurements on uniform oxides).

fully uncorrelated (correlation coefficient $r=0.0$), while the standard deviation of the ρ_{sh} -distribution remains below 3%.

Table 1. Variations in ρ_{sh} for $T_{ox}=7.5$ nm.

| Implant | RTA | $\langle\rho_{sh}\rangle$ | $d\rho_{sh}/dT_{ox}$ |
|----------------------------------|-------------------|---------------------------|----------------------|
| 1 keV B 1E15/cm ² | 1000 °C 10 sec | 924 Ω | 39 Ω/Å |
| 1 keV B 1E15/cm ² | 1020 °C 10 sec | 762 Ω | 41 Ω/Å |
| 500 eV B 3E15/cm ² | 1000 °C 10 sec | 3.6 kΩ | 366 Ω/Å |
| 500 eV B 3E15/cm ² | 1020 °C 10 sec | 2.9 kΩ | 277 Ω/Å |

The fitted slope in Fig. 3 shows that ρ_{sh} varies by as much as 277 Ω/Å (~10%/Å). Table 1 summarizes the average value, $\langle\rho_{sh}\rangle$, and variation, $d\rho_{sh}/dT_{ox}$, of the sheet resistance for different implant and annealing conditions. The relative variation in ρ_{sh} decreases from ~10 to ~5%/Å when going from 0.5 to 1 keV implants. This is because a smaller fraction of the implanted B is contained in the oxide layer at higher energies, making the junction formation less sensitive to T_{ox} . Likewise, the ρ_{sh} -variations are expected to be less pronounced for higher implant doses or thinner oxides (see Fig. 2).

To investigate the origin of the variations in ρ_{sh} , SIMS profiling was performed on 5 positions of the wafer analyzed in Fig. 3, representing a total shift in T_{ox} of ~5 Å. Figure 4 confirms that the level of B incorporated into Si varies by almost a factor of 2 over the wafer, consistent with the measured changes in ρ_{sh} . The junction depth, on the other hand, changes by at most 20% in response to the T_{ox} variations.

The above observations have important implications for the manufacturability of PMOS transistors. For instance, source/drain extensions are generally implanted through thin oxide layers that

remain after the poly-gate etching and reoxidation steps (typically, $T_{ox} \sim 3-6$ nm for $0.13 \mu\text{m}$ CMOS). For low-energy B implants, small thickness changes arising from variations in the etching and/or oxidation rates have a severe impact on the junction profiles obtained after annealing. Although the impact on junction depth (and thereby short-channel effects) is relatively small (see Fig. 4), the induced variations in ρ_{sh} will strongly affect the transistor drive current through parasitic resistance variations. Therefore, the thickness of screening oxides needs to be controlled to within a few Å in order to suppress undesired variations in transistor performance.

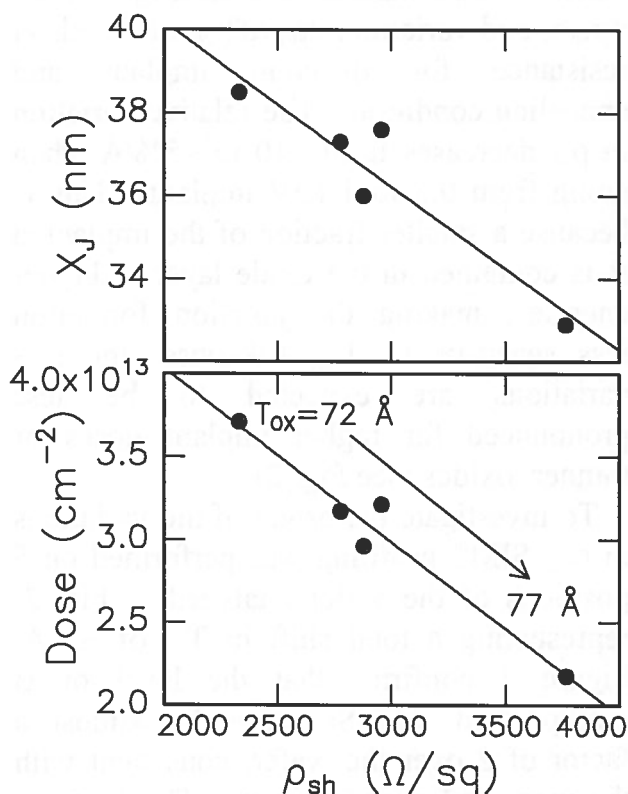


Figure 4. SIMS measurement of junction depth (top) and integrated B dose in Si (bottom) vs. sheet resistance. The data were obtained from 5 different positions on a single wafer with non-uniform screening oxide.

4. Conclusions

We have investigated the influence of screening oxides on the formation of shallow junctions using low energy B implantation. The trapping of B in the surface oxides eliminates B clustering in the peak of the profile, and leads to a reduction in both the junction depth and the active B level in the Si region. Yet, the trade-off between X_j and ρ_{sh} is not affected as long as the implanted dose is adjusted to compensate for B trapping in the screening oxide. For a fixed implant dose and energy, minute variations in the oxide thickness have a large influence on ρ_{sh} . Hence, the presence of screening oxides in transistor fabrication requires ultimate control over the oxide thickness in order to ensure reproducible transistor performance.

The authors would like to acknowledge J.B.F. aan de Stegge and his team for tuning the oxidation recipes, and F. Roozeboom for performing part of the RTA steps. This work was performed as part of the EC Ultra Project (ESPRIT E23806).

5. References

- [1] E.J.H. Collart, K. Weemers, D.J. Gravesteijn, and J.G.M. van Berkum, *J. Vac. Sci. Tech. B*, vol.16 (1998), pp.280-5.
- [2] A. Agarwal, A.T. Fiory, H.-J. Gossmann, C.S. Rafferty, and P. Frisella, *Mat. Sci. in Semicond. Proc.*, vol. 1 (1999), pp. 237-242.
- [3] S. Shishiguchi, A. Mineji, T. Yasunaga, and S. Saito, *Tech. Digest VLSI-1998*, pp. 135-136.
- [4] J. Schmitz, M. van Gestel, P.A. Stolk, Y.V. Ponomarev, F. Roozeboom, J.G.M. van Berkum, P.C. Zalm, and P.H. Woerlee, *Tech. Digest IEDM-1998*, pp. 1009-1012.